SUPPLEMENTARY INFORMATION

PEGDA Hydrogel Structure from Semi-Dilute Concentrations: Insights from Experiments and Molecular Simulations

Jomary Mercado-Montijo,[a] Dylan M. Anstine,[ab] Shalini J. Rukmani,[ab] Coray M. Colina [abc] and Jennifer S. Andrew [a]

[a] Department of Materials Science and Engineering, University of Florida, Gainesville, Florida 32611, United States.
[b] George and Josephine Butler Polymer Research Laboratory, University of Florida, Gainesville, Florida 32611, United States.
[c] Department of Chemistry, University of Florida, Gainesville, Florida 32611, United States

Correspondence
jandrew@mse.ufl.edu
colina@chem.ufl.edu

Table S1. PEG and water characteristic constant values

Parameter	Description	Value
χ	Flory Huggin's PEG-water interaction constant	0.426
V_1	Molar volume of water	18 cm^3/mol
ρ_d	Dry density of PEG	1.12 g/cm^3
M_r	Molecular weight of PEG repeating unit	44 g/mol
C_∞	PEG characteristic ratio	4
λ	PEG backbone bond factor	3
l	Weighted mean bond length for PEG repeating unit	0.1464 nm

Table S2. Summary of the number of water molecules in each simulated hydrogel sample.

	Number of Water Molecules / Simulation Cell	
Conc. (wt. %)	4.8 kDa	10 kDa
15	5849	17621
20	4431	14784
25	4003	12812
30	3382	11392
35	3147	9646
40	3015	9242
50	2735	8066
60	2337	7396
70	2121	-

Table S3. Summary of the average number density of polymer chain-chain contacts over each 200 ns simulation trajectory

	Number density of chain-chain contacts ($\mathring{A}^{-3}$)	
Conc. (wt. %)	4.8 kDa	10 kDa
15	0.155 (0.011)	0.109 (0.002)
20	0.201 (0.017)	0.127 (0.003)
25	0.214 (0.013	0.150 (0.003)
30	0.257 (0.022)	0.161 (0.004)
35	0.274 (0.018)	0.188 (0.004)
40	0.270 (0.014)	0.197 (0.006)
50	0.298 (0.020)	0.220 (0.004)
60	0.372 (0.041)	0.234 (0.004)
70	0.410 (0.050)	-

A chain-chain contact is defined by the number of instances where a polymer atom is within 3.5 Å of another polymer atom. The cutoff was chosen to be similar to the sigma parameters from the applied force field. The exact choice of cutoff has a minimal influence on the relative comparison between concentrations and only affects the total number of contacts. Numbers in parenthesis denote the standard deviation over the 200 ns trajectory.

NOTE: Reference error in main manuscript. Look at **Table S3** for the calculated number density of chain–chain contacts in PEGDA hydrogels.

Table S4. Summary of the maximum pore diameter peaks across all simulated hydrogel samples and the ratio between macromer molar masses.				
	4.8 kDa	10 kDa	10 kDa / 4.8 kDa	
Conc. (wt. %)	pore diameter (nm)	pore diameter (nm)	pore peak ratio	uncertainty
15	3.58	5.37	1.50	0.18
20	3.05	4.71	1.55	0.22
25	2.82	4.54	1.61	0.22
30	2.61	4.17	1.60	0.22
35	2.60	3.61	1.39	0.18
40	2.54	3.82	1.51	0.22
50	2.37	3.53	1.49	0.20
60	2.30	3.19	1.39	0.19
70	2.26	-	-	-
The ratio of maximum pore diameter peaks is approximately equal to the ratio of $\sqrt{n}_{10\,kDa}/\sqrt{n}_{4.8\,kDa} = 1.46$, where n is the number of backbone bonds per macromer chain.				

Table S5. Full Width at Half Maximum of PEGDA computational hydrogel models across a range of initial solution concentrations (conc.).

Conc. (wt. %)	4.8 kDa (Å)	10 kDa (Å)
15	12.83	17.43
20	12.36	17.95
25	11.93	16.55
30	10.56	15.57
35	10.66	15.06
40	9.51	15.41
50	8.71	13.70
60	8.91	13.74
70	8.1	-

The full width at half maximum is a measure of the breadth of a unimodal distribution, and therefore, is an effective measure of the average pore dynamics.

Additional viscosity measurements – Overlap Concentration C*

Additional viscosity measurements were obtained using micro-rheology. Briefly, carboxylated polystyrene particles (radius ~0.8 um) were suspended with a total mass fraction of 0.04% in PEGDA solutions and their trajectory was tracked using microscopy. The viscosity was calculated from Stokes-Einstein equation by estimating the diffusion coefficient of the particles in solution.
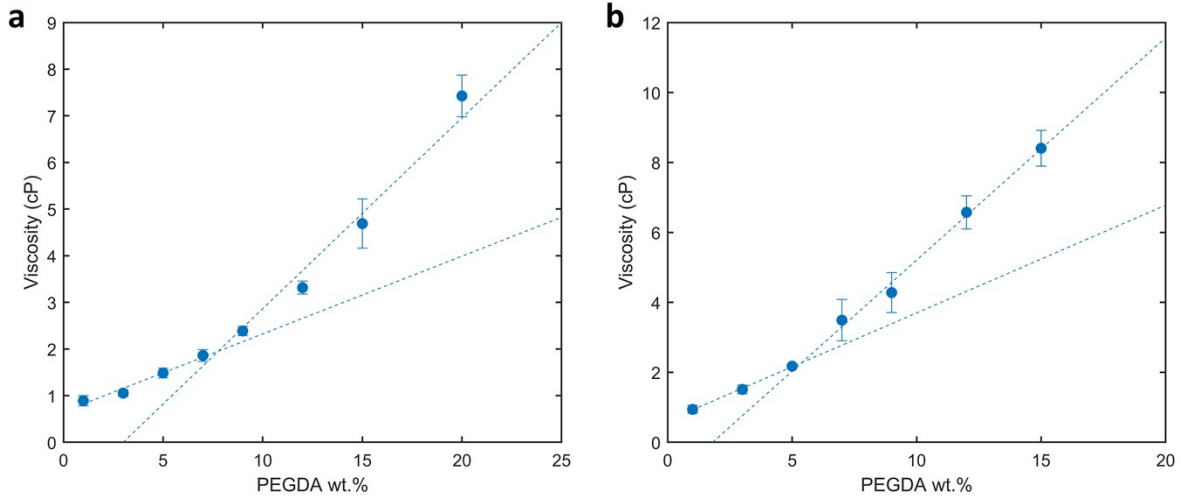
Figure S1. Viscosity plots for a) PEGDA 4.8 and b) 10 kDa solutions from micro-rheology measurements. Inflection point of each corresponds to an overlap concentration of 8.3 and 5.4 wt.% for 4.8 and 10 kDa, respectively.
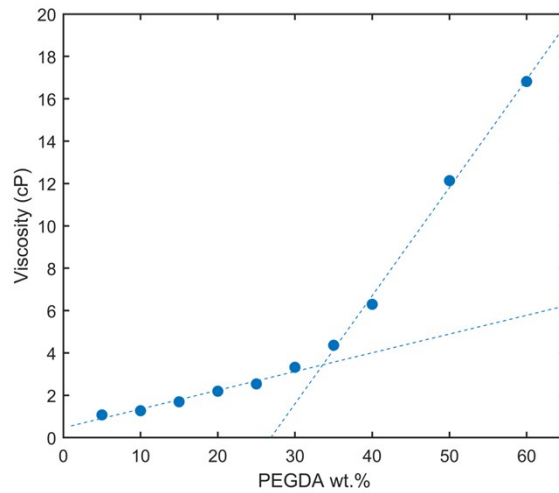
Figure S2. Viscosity plot for PEGDA 700 Da solutions from micro-rheology measurements. Inflection point corresponds to an overlap concentration of 33.6 wt.%.

End-to-end distance mesh size
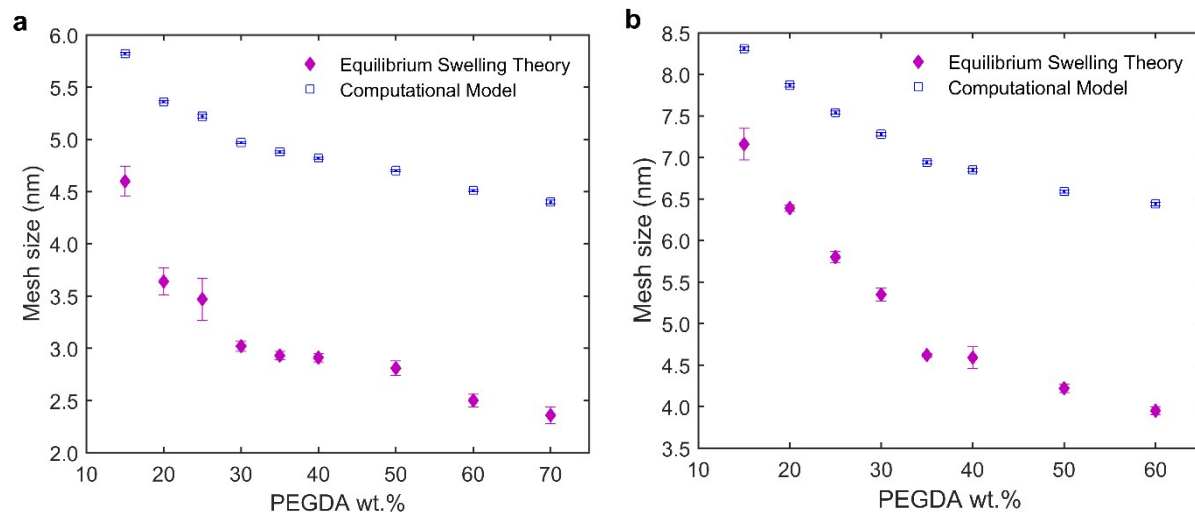
Figure S3. Mesh size as the end-to-end distance between crosslinks between equilibrium swelling theory measurements from an effective hydrogel representation (◆) and from the computational model (□) for a) PEGDA 4.8 kDa and b) PEGDA 10 kDa.
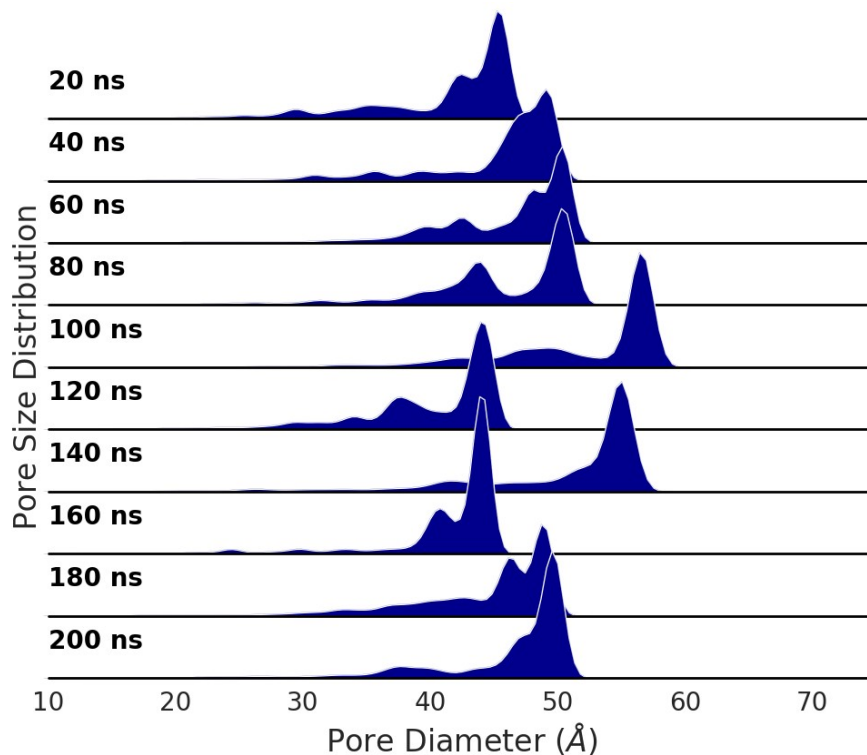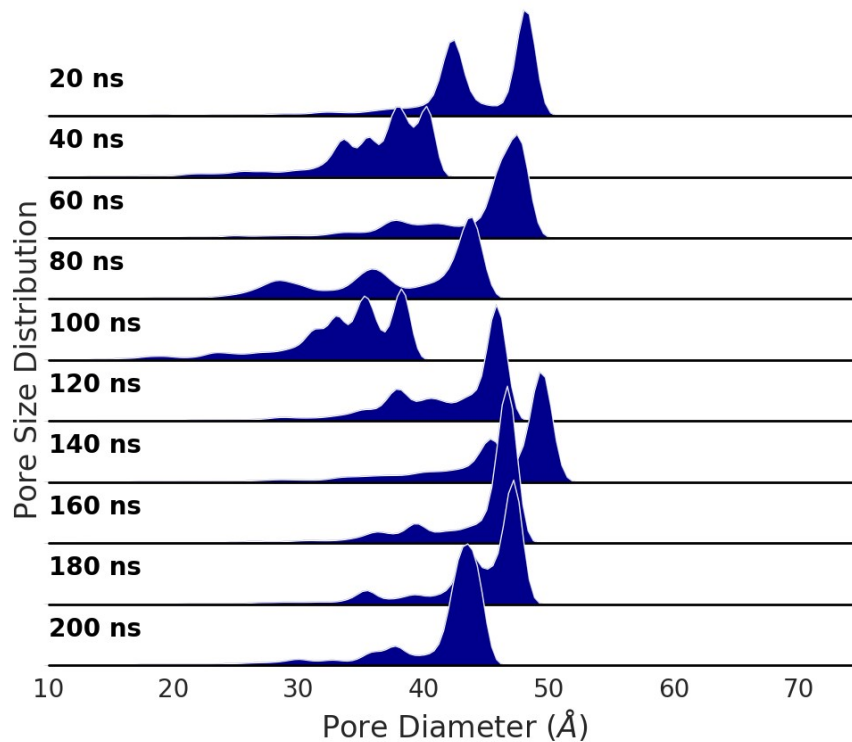
Dynamic pore size distribution
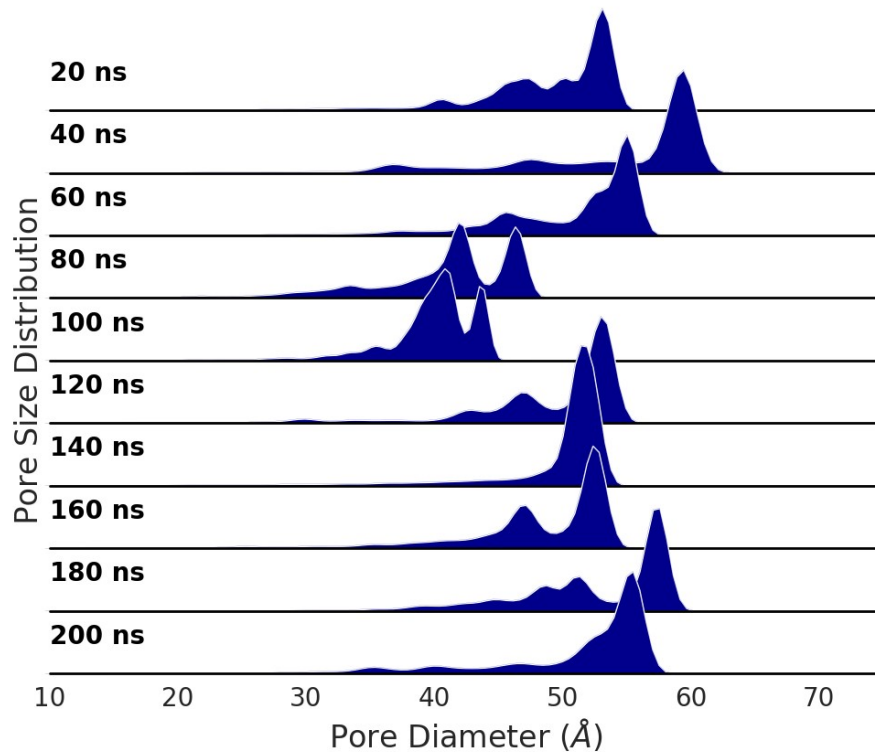
Figure S4 Dynamic pore size distributions (DPSDs) for 10 kDa computational hydrogel models corresponding to a pre-gel solution concentration of 20 wt%. A small smoothing factor has been applied for ease of visualization.
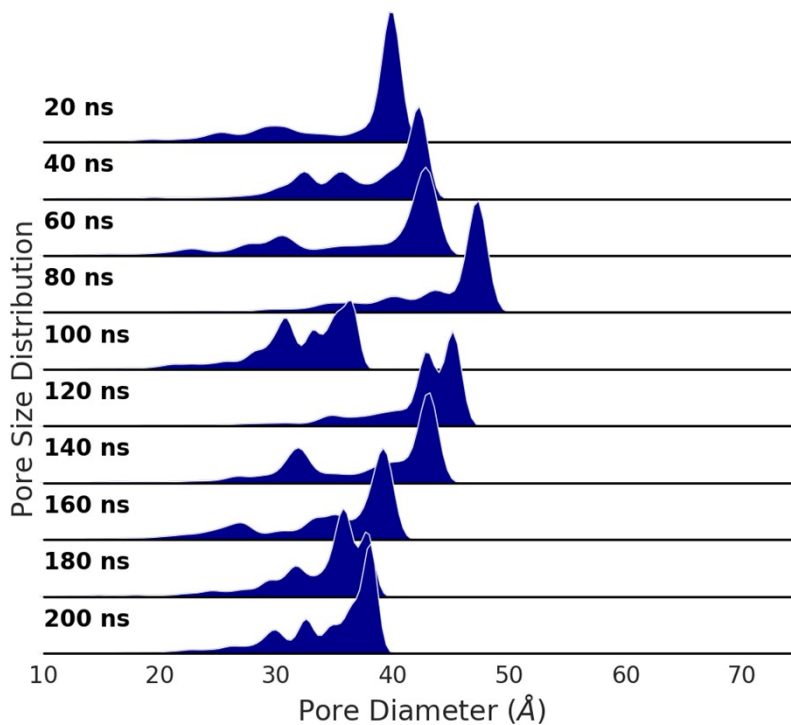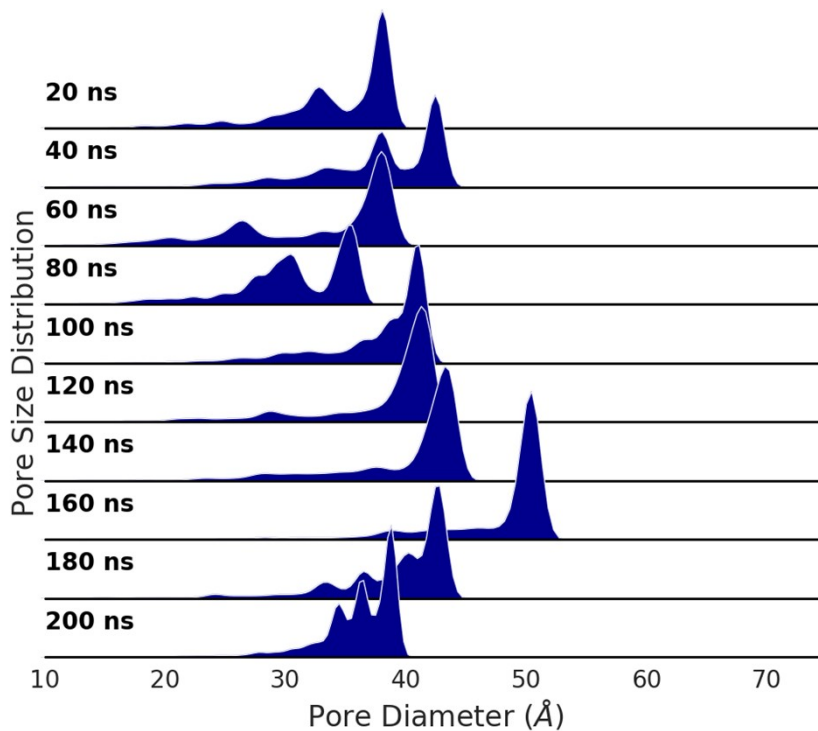
Figure S5 Dynamic pore size distributions (DPSDs) for 10 kDa computational hydrogel models corresponding to a pre-gel solution concentration of 25 wt%. A small smoothing factor has been applied for ease of visualization.
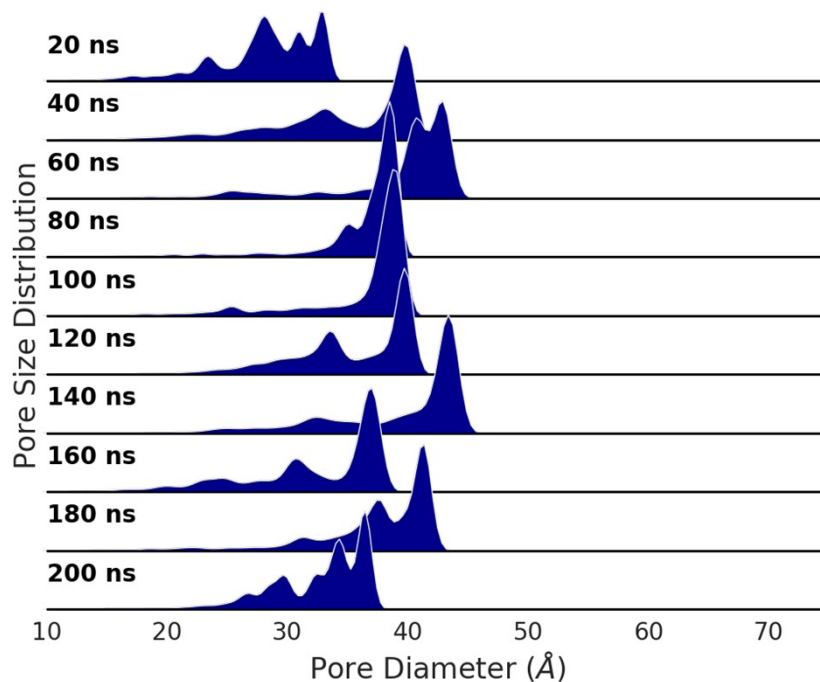

Figure S6 Dynamic pore size distributions (DPSDs) for 10 kDa computational hydrogel models corresponding to a pre-gel solution concentration of 30 wt%. A small smoothing factor has been applied for ease of visualization.

Figure S7 Dynamic pore size distributions (DPSDs) for 10 kDa computational hydrogel models corresponding to a pre-gel solution concentration of 35 wt%. A small smoothing factor has been applied for ease of visualization.
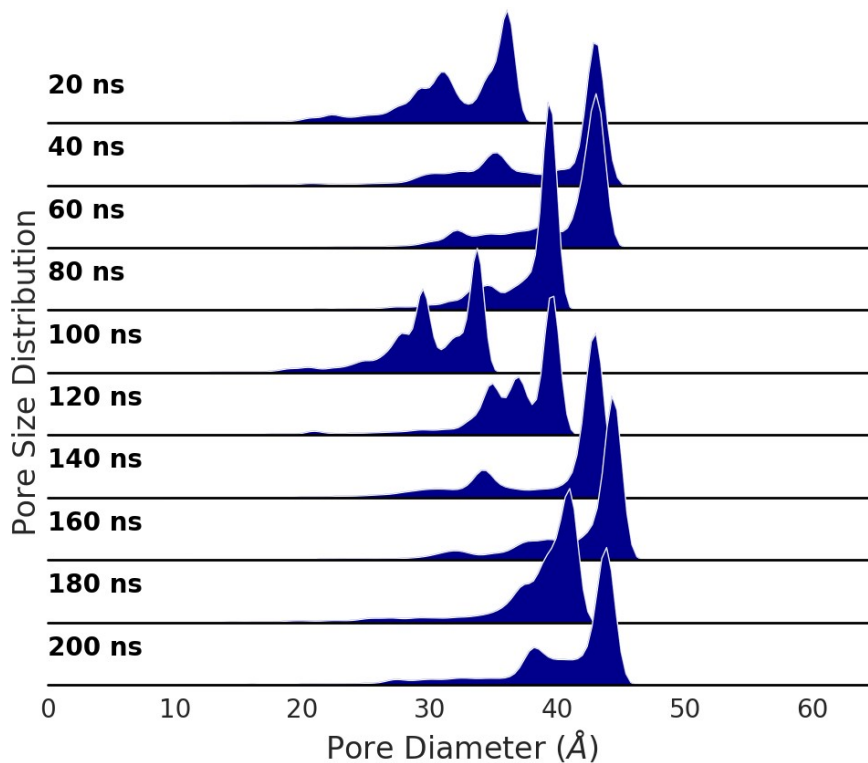

Figure S8 Dynamic pore size distributions (DPSDs) for 10 kDa computational hydrogel models corresponding to a pre-gel solution concentration of 40 wt%. A small smoothing factor has been applied for ease of visualization.
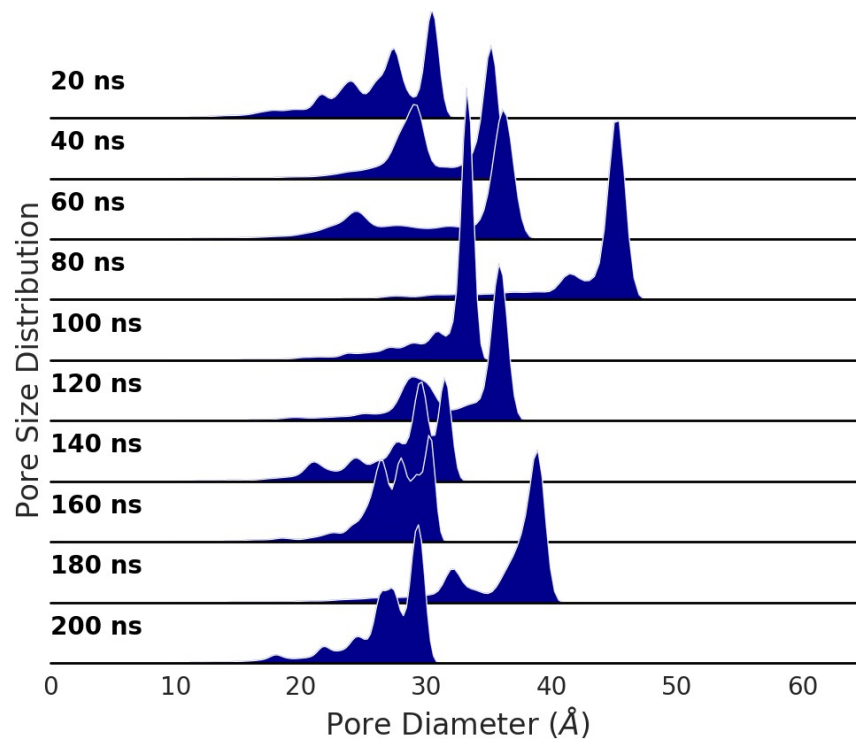
Figure S9 Dynamic pore size distributions (DPSDs) for 10 kDa computational hydrogel models corresponding to a pre-gel solution concentration of 50 wt%. A small smoothing factor has been applied for ease of visualization.
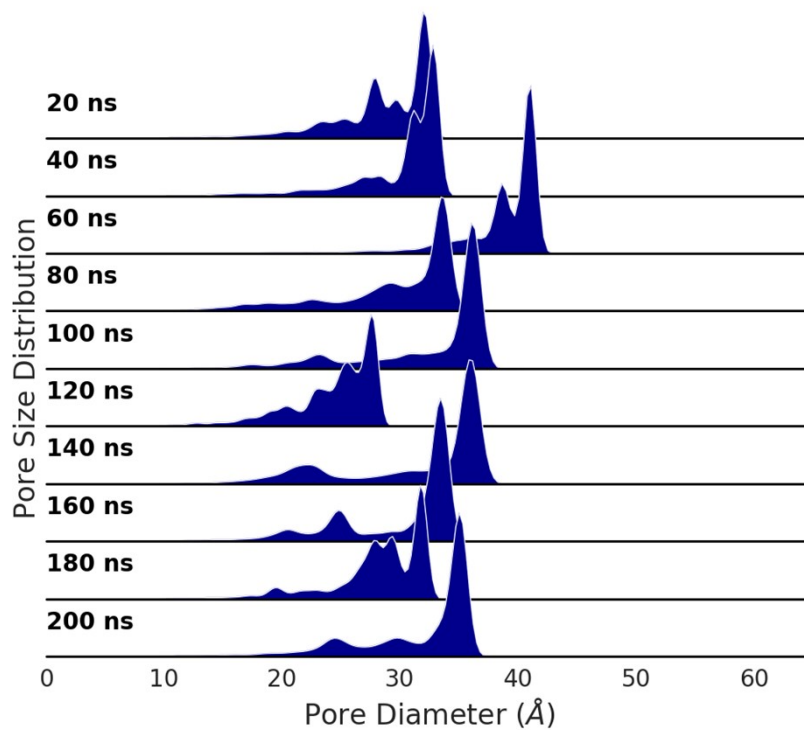

Figure S10 Dynamic pore size distributions (DPSDs) for 4.8 kDa computational hydrogel models corresponding to a pre-gel solution concentration of 15 wt%. A small smoothing factor has been applied for ease of visualization.

Figure S11 Dynamic pore size distributions (DPSDs) for 4.8 kDa computational hydrogel models corresponding to a pre-gel solution concentration of 20 wt%. A small smoothing factor has been applied for ease of visualization.
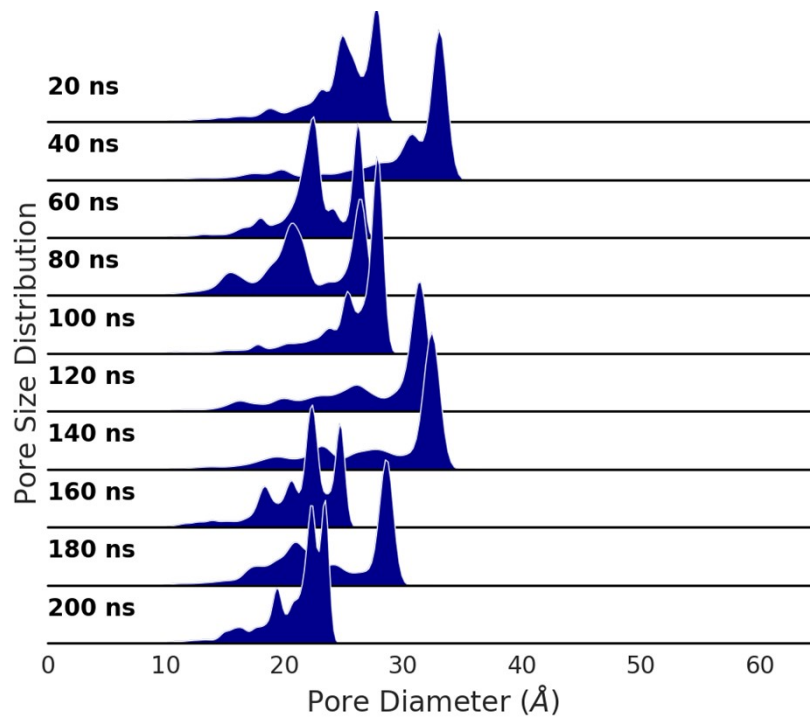

Figure S12 Dynamic pore size distributions (DPSDs) for 4.8 kDa computational hydrogel models corresponding to a pre-gel solution concentration of 25 wt%. A small smoothing factor has been applied for ease of visualization.
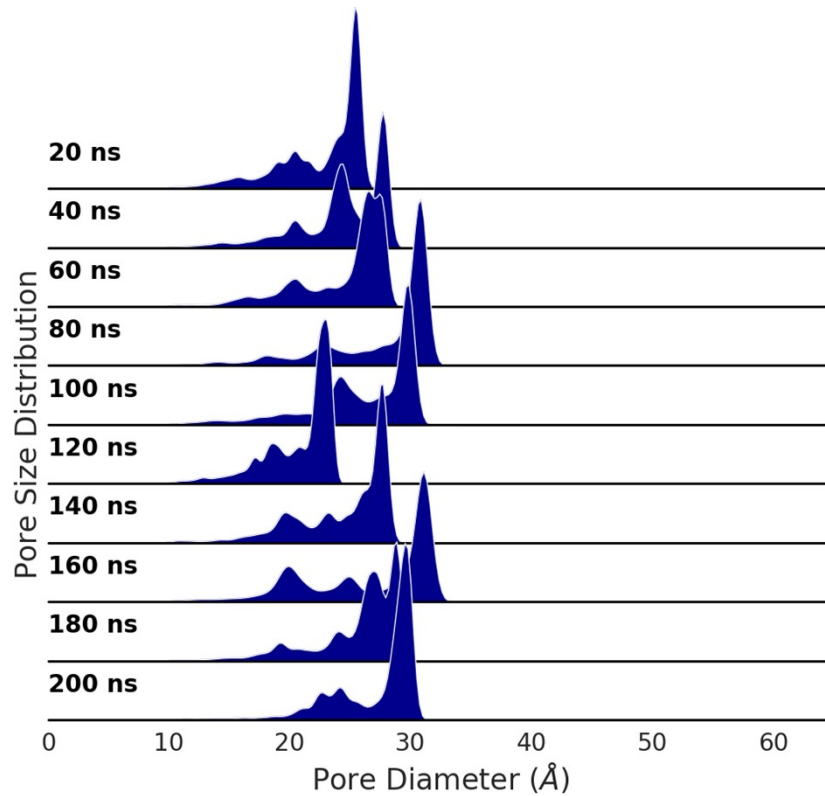
Figure S13 Dynamic pore size distributions (DPSDs) for 4.8 kDa computational hydrogel models corresponding to a pre-gel solution concentration of 30 wt%. A small smoothing factor has been applied for ease of visualization.
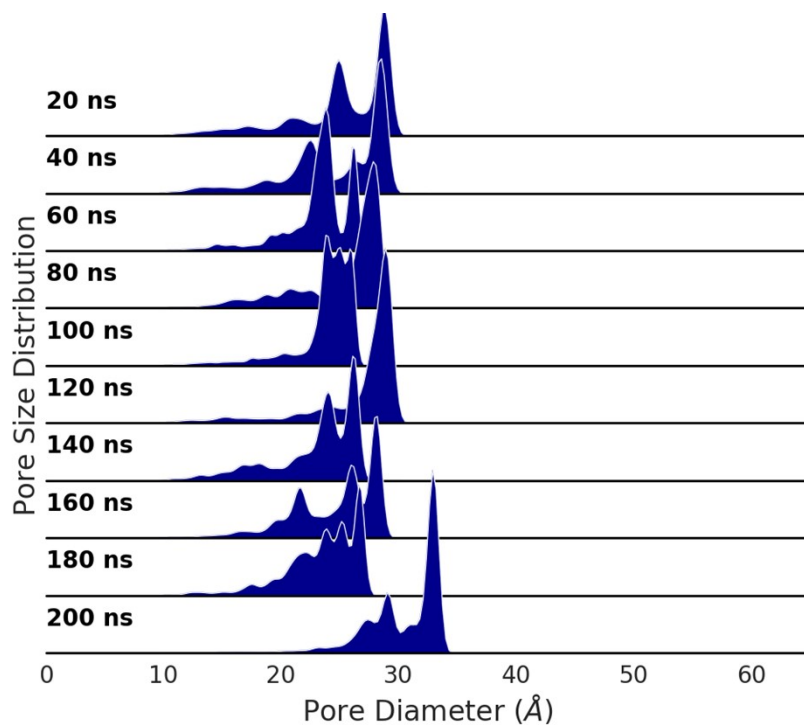

Figure S14 Dynamic pore size distributions (DPSDs) for 4.8 kDa computational hydrogel models corresponding to a pre-gel solution concentration of 35 wt%. A small smoothing factor has been applied for ease of visualization.

Figure S15 Dynamic pore size distributions (DPSDs) for 4.8 kDa computational hydrogel models corresponding to a pre-gel solution concentration of 40 wt%. A small smoothing factor has been applied for ease of visualization.
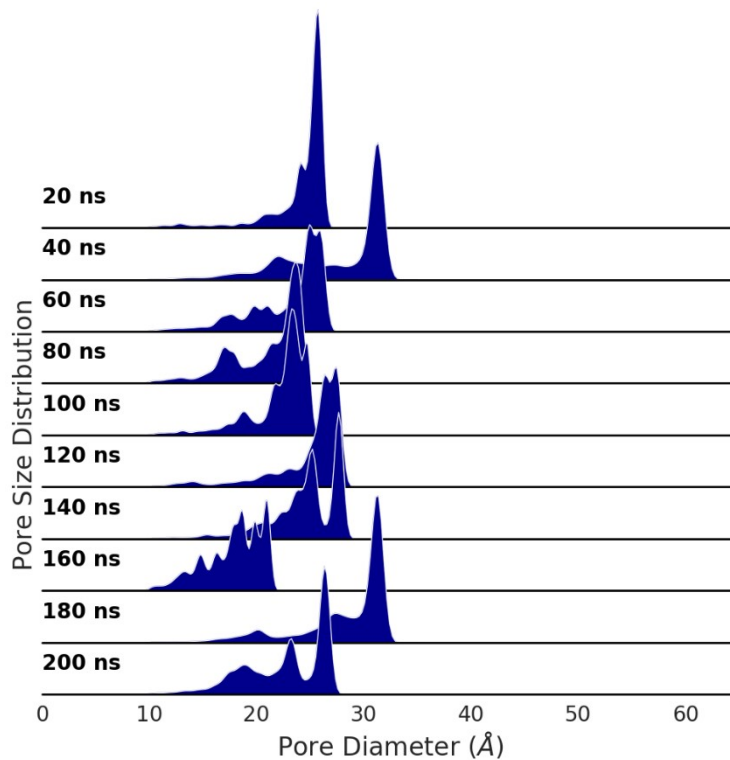

Figure S16 Dynamic pore size distributions (DPSDs) for 4.8 kDa computational hydrogel models corresponding to a pre-gel solution concentration of 50 wt%. A small smoothing factor has been applied for ease of visualization.
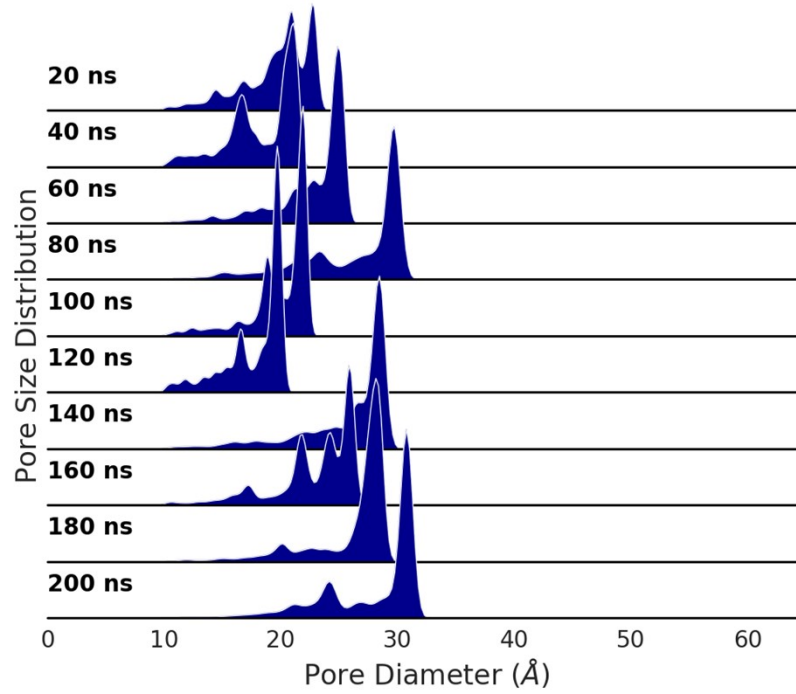
Figure S17 Dynamic pore size distributions (DPSDs) for 4.8 kDa computational hydrogel models corresponding to a pre-gel solution concentration of 60 wt%. A small smoothing factor has been applied for ease of visualization.

Figure S18 Dynamic pore size distributions (DPSDs) for 4.8 kDa computational hydrogel models corresponding to a pre-gel solution concentration of 70 wt%. A small smoothing fact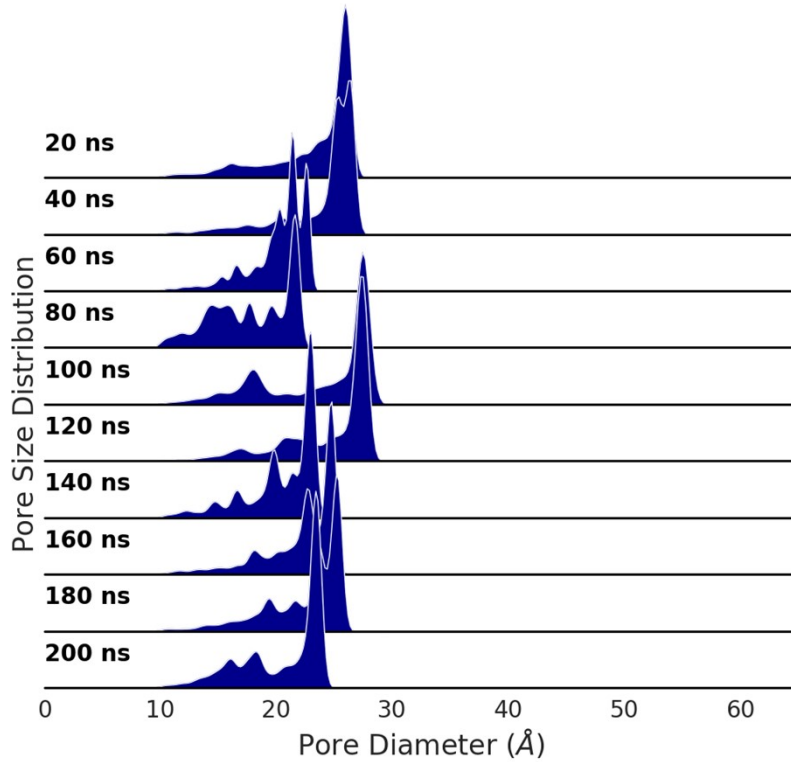or has been applied for ease of visualization.